Remote Sensing of Environment 124 (2012) 310–320

Contents lists available at SciVerse ScienceDirect

Remote Sensing of Environment

journal homepage: www.elsevier.com/locate/rse

Combining object-based texture measures with a neural network for vegetation mapping in the Everglades from hyperspectral imagery

Caiyun Zhang *, Zhixiao Xie

Department of Geosciences, Florida Atlantic University, 777 Glades Road, Boca Raton, FL 33431, USA

ARTICLE INFO

Article history:
Received 25 February 2012
Received in revised form 16 May 2012
Accepted 19 May 2012
Available online 17 June 2012

Keywords:
Texture analysis
Object-based image analysis
Neural network
Hyperspectral imagery
Everglades

ABSTRACT

An informative and accurate vegetation map for the Greater Everglades of South Florida is in an urgent need to assist with the Comprehensive Everglades Restoration Plan (CERP), a $10.5-billion mission to restore the south Florida ecosystem in 30+ years. In this study, we examined the capability of fine spatial resolution hyperspectral imagery collected from Airborne Visible/Infrared Imaging Spectrometer (AVIRIS) for vegetation mapping in the Everglades. In order to obtain an efficient and accurate procedure for vegetation discrimination, we developed a neural network classifier first and then combined the object-based texture measures with the classifier to examine the contribution of the spatial information for vegetation mapping. The neural network is capable of modeling the characteristics of multiple spectral and spatial signatures within a class by an internally unsupervised engine and characterizing spectral and spatial differences between classes by an externally supervised system. The designed procedure was tested in a portion of the Everglades. An object-based vegetation map was generated with an overall classification accuracy averaged 94% and a kappa value averaged 0.94 in discriminating 15 classes. The results are significantly better than those obtained from conventional classifiers such as maximum likelihood and spectral angle mapper. The study illustrates that combining object-based texture measures in the neural network classifier can significantly improve the classification. It is concluded that fine spatial resolution hyperspectral data is an effective solution to accurate vegetation mapping in the Everglades which has a rich plant community with a high degree of spatial and spectral heterogeneity.

1. Introduction

The Greater Everglades of South Florida has been designated as an International Biosphere Reserve, a World Heritage Site, and a Wetland of International Importance due to its unique combination of hydrology and water-based ecology that supports many threatened and endangered species (Davis et al., 1994). However, human activities in the past century has severely altered and threatened this natural ecosystem. This has led to a variety of environmental issues in south Florida (McPherson & Halley, 1996). To protect this valuable resource, Congress authorized a project known as Comprehensive Everglades Restoration Plan (CERP) in 2000 to restore south Florida's natural ecosystem, while maintaining urban and agricultural water supply and flood control over this region. CERP is a $10.5 billion mission that is expected to take 30 or more years to complete (CERP, 2012, http://www.evergladesplan.org/). With such a high amount of funds planned for restoration of this unique environment, emphasis has been placed on developing a thorough understanding of how past changes in hydrology have affected Everglades plant and animal communities and what will be changed when the CERP is completed. Detailed and accurate spatial data such as vegetation maps are key factors required to document change in the Everglades (Doren et al., 1999; Welch et al., 1999).

Remote sensing has been frequently cited as a cost-effective and labor-saving technique for monitoring and mapping wetlands. A wide range of studies has been undertaken in a variety of wetland environments (Adam et al., 2010). To generate detailed and accurate vegetation maps, researchers traditionally adopt large-scale aerial photographs assisted with visual interpretation techniques (Madden et al., 1999; Rutchey & Vilchek, 1999). This conventional approach is time-consuming, costly, and requires experienced specialists. The results may be inconsistent if done by different analysts. With the availability of digital images, it has been anticipated that this procedure can be superseded by semi-automated or automated digital image analysis approaches that promise greater efficiency and consistency. A number of efforts have been made for this purpose by using data collected either from multispectral or hyperspectral sensors (Adam et al., 2010). Hyperspectral sensors are more powerful in vegetation mapping due to their rich spectral contents. The application of this type of data is the primary research interests in the past decade. Studies in wetland vegetation characterization using hyperspectral sensors can be grouped into two categories. The first category is the

* Corresponding author. Tel.: +1 561 297 2648.
E-mail address: czhang3@fau.edu (C. Zhang).

0034-4257/$ – see front matter © 2012 Elsevier Inc. All rights reserved.
doi:10.1016/j.rse.2012.05.015

application of sensors with a low spatial resolution (i.e. 20–30 m or larger), such as EO-1/Hyperion and high altitude Airborne Visible/Infrared Imaging Spectrometer (AVIRIS) (e.g., Hirano et al., 2003; Pengra et al., 2007; Rosso et al., 2005). Limitations of these sensors include the coarse spatial resolution and complexity of image processing procedures (Hirano et al., 2003). The second category is the employment of hyperspectral data with a fine spatial resolution (i.e. 4 m or smaller), such as imagery collected from low altitude Compact Airborne Spectrographic Imager (CASI) and AVIRIS (Artigas & Yang, 2005; Held et al., 2003; Hunter & Power, 2002; Jollineau & Howarth, 2008; Kamal & Phinn, 2011; Li et al., 2005; Schmidt et al., 2004). So far they are the best remotely sensed data for vegetation mapping with suitable spectral and spatial resolution.

A challenge in the application of fine spatial resolution hyperspectral imagery in wetland environments is the shortage of effective processing procedures which could take advantage of its fine spatial and spectral resolution. Most researchers concentrate on the examination of endmember-based approaches, such as the spectral angle mapper (SAM) and linear spectral unmixing, which are specifically designed to extract information from hyperspectral imagery (e.g., Artigas & Yang, 2005; Belluco et al., 2006; Harken & Sugumaran, 2005; Held et al., 2003; Hirano et al., 2003; Hunter & Power, 2002; Jollineau & Howarth, 2008; Li et al., 2005; Rosso et al., 2005; Schmidt et al., 2004). These approaches may not achieve the expected results in complex wetlands due to the difficulties inherent in determining hyperspectral endmembers, a shortage of comprehensive spectral libraries for different wetland plants, and the violation of the assumption in the algorithms that only one spectral representative (i.e. the endmember) exists for each vegetation type. In addition, most of these researches did not consider the rich spatial information of the data, although it has been proved useful in image classification (De Jong & van der Meer, 2004). Innovative new processing techniques with the capability to solve the above problems and generate more informative and accurate wetland vegetation maps from fine spatial resolution hyperspectral data are expected.

The literature has demonstrated that neural network approaches are attractive options in remote sensing image processing. These techniques have been extensively employed to analyze multispectral images and often shown more accurate results than other classification approaches (Atkinson & Tatnall, 1997; Mas & Flores, 2008). More recently Adam et al. (2010) reviewed the multispectral and hyperspectral remote sensing for mapping wetland vegetation, and conclude that the neural networks are valuable in mapping wetland vegetation types. However, their applications in hyperspectral data analysis are limited because they are assumed to be computationally demanding for processing large datasets. Efficient and effective neural networks for analyzing a large volume of hyperspectral data are desired.

The literature has also illustrated that object-based image analysis methods are desirable in processing high spatial resolution remotely sensed data. These techniques decompose an image scene into relatively homogeneous objects or segments and permit the analysts to use both spectral and spatial information for image classification (Jensen, 2005). Blaschke (2010) reviewed these techniques for remote sensing and concludes that they are effective approaches in classification of high spatial resolution data. Several researchers have evaluated these approaches for wetland mapping and found that they can generate better accuracy compared with the traditional pixel-based methods (e.g., Harken & Sugumaran, 2005; Kamal & Phinn, 2011).

Texture analysis has been of great interest in remote sensing for more than three decades with attempt to incorporate spatial properties in classification. A recent review by Warner (2011) concludes that texture measures are useful but challenging in determining the optimal kernel scale, an important parameter in texture analysis. The object-based texture analysis methods may overcome these challenges by locally adapting the kernel size over the image. A recent study by Batista and Haertel (2010) demonstrate that by calculating texture over semantically meaningful objects, rather than arbitrarily sized square kernels, the issue of separating between- and within-class texture may be resolved. Kim et al. (2009) demonstrate a substantial increase in classification accuracy for mapping forest types using the object-based texture measures.

Neural networks, object-based image analysis, and texture analysis are popular techniques in image classification, as evidenced by the review papers (Blaschke, 2010; Mas & Flores, 2008; Warner, 2011). These approaches have been primarily tested for multispectral data processing. A combination of them for hyperspectral data analysis is limited. An effective integration of these three techniques for vegetation mapping in complex wetland environment to analyze fine spatial resolution hyperspectral imagery is even scarcer. To this end, the aim of this study is to develop an efficient and accurate processing procedure to analyze high spatial resolution hyperspectral data for vegetation mapping in the Everglades. In order to take advantage of the fine spatial and spectral information offered by this type of data, the procedure extracts the object-based texture measures first and then integrates these texture measures with a designed neural network classification. Finally, an object-based vegetation map can be generated. The object-based map is more informative and useful than a traditional pixel-based map which may be noisy if the wetlands have a high degree of spatial heterogeneity and diverse vegetation types.

2. Study area and data

The study area is a portion of Caloosahatchee River watershed in the Everglades (Fig. 1). The Everglades is a vast subtropical wetland that occupies most of the southern peninsula of Florida and extends southward from Lake Okeechobee to Florida bay. Lake Okeechobee serves as the “water heart” for the Everglades, and the Caloosahatchee River functions as a primary canal that conveys basin runoff and regulatory releases from Lake Okeechobee. Caloosahatchee watershed is an important environmental and economic resource in the Everglades. The hydrology of this region has been severely changed because many canals were constructed along the banks of the river to support the agricultural communities associated with the river. “Get the water right” in the Caloosahatchee watershed is a key component in CERP. Response of the plant community in this region is a crucial indicator of the restoration success and detailed vegetation maps can guide the path of restoration. The selected study area is a mosaic of common wetland vegetation community, agricultural plant community, exotic species, water bodies, and man-made concrete features. This is a challenging site for vegetation characterization from remote sensing.

Data sources used in this study include the hyperspectral imagery collected by Airborne Visible/Infrared Imaging Spectrometer (AVIRIS) and reference data manually interpreted from National Aerial Photography Program (NAPP) color infrared (CIR) images. AVIRIS is a premier instrument in the realm of Earth Remote Sensing. It delivers calibrated hyperspectral images in 224 contiguous spectral channels with wavelengths from 400 to 2500 nm. The South Florida Water Management District (SFWMD) collected the AVIRIS data over the Caloosahatchee watershed on November 16, 1998 through coordination with the Jet Propulsion Laboratory (JPL) at the California Institute of Technology. The instrument was on board the National Aeronautics & Space Administration (NASA)'s Twin Otter aircraft with a low flying altitude. This resulted in an acquisition of high spatial resolution hyperspectral data with a pixel size of 4.0 m. A natural color composite for the selected study area is shown in Fig. 1. JPL conducted the geometrical correction for the deliverables. The SFWMD also provided the reference data for this study. The reference data were photointerpreted from 1999 NAPP CIR 1:40, 000 aerial photography and classified using the SFWMD modified Florida Land Use, Land Cover Classification System. Features were stereoscopically interpreted

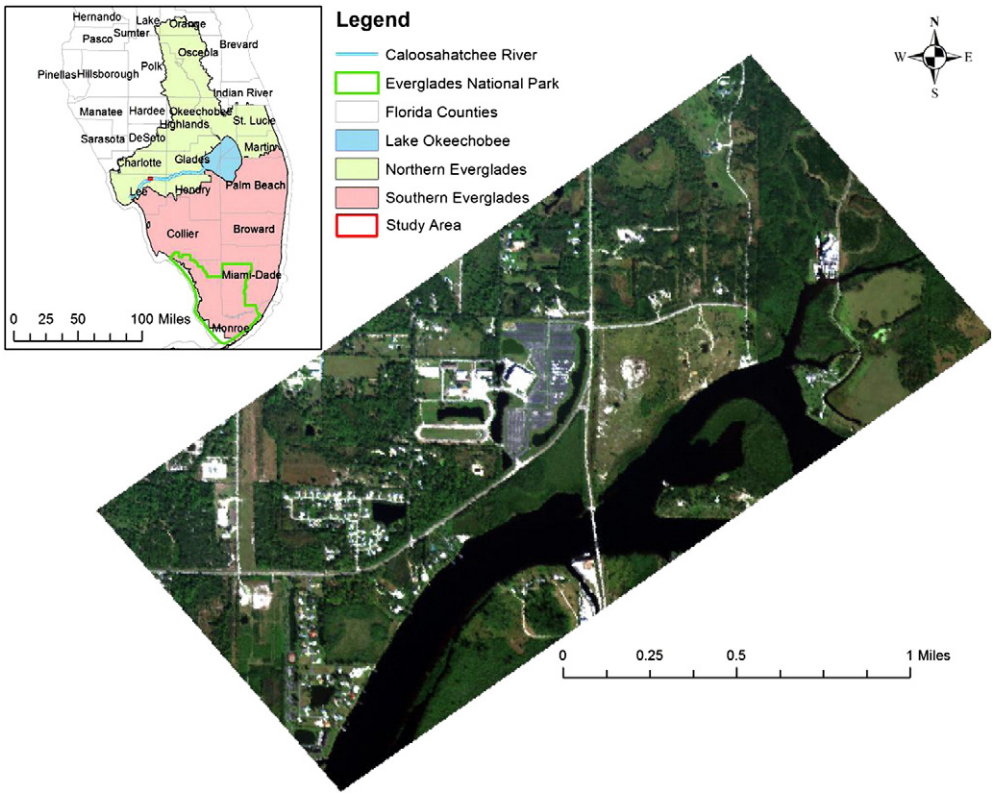

Fig. 1. Map of Greater Everglades, Caloosahatchee River, and a color composite generated from the hyperspectral imagery for the study area.

using a stereo plotter and calibrated from field surveys through a project known as "Land Cover/Land Use Mapping Project" conducted at the SFWMD. In the project, the data was compiled on screen over corresponding U.S. Geological Survey (USGS) Digital Orthophoto Quadrangles (DOQs). The positional accuracy of the data meets the National Map Accuracy Standards (NMAS) adopted by USGS. The SFWMD reports the dataset has a minimum accuracy of 90%. A total of 2580 reference samples were spatially randomly selected over the study area using a strategy called equal sample rate in which a fixed percentage of samples are randomly selected for each class. The number of reference samples for each class was calculated based on the segmentation result and the SFWMD reference data. The random selection scheme can minimize the effect of spatial correlation of data and improve the spectral variability of each class (Campbell, 1996). The number of selected samples for each vegetation type is listed in Table 1. To further improve the accuracy of the selected samples, we overlaid them first on the hyperspectral imagery that was georeferenced by the DOQs, and then visually validated each sample and manually corrected misclassified samples. For the selected study area, a total of 15 vegetation covers were found; they are dry prairie, improved pastures, groves, fruit orchard, upland shrub and brush, pine flatwood, upland hardwood forest, Brazilian pepper (exotic species), Melaleuca (exotic species), hardwood/coniferous mix, mangrove swamp, mixed wetland hardwoods, mixed shrub, cypress, and freshwater marshes. These vegetation types need to be discriminated from the collected hyperspectral imagery using the digital image analysis procedure.

3. Methodology

3.1. Procedure design

In order to generate an informative and accurate vegetation map from fine spatial resolution hyperspectral imagery, multiple data processing steps are required. They are summarized in Fig. 2 and described as below.

1) Noisy band removal
   Noisy bands are unavoidable in hyperspectral data and need to be eliminated first. Visual examination of the data revealed 97 noisy bands which should be dropped for further analysis. The remained 127 bands (i.e. bands 4–6, 10–13, 15, 18, 20–21, 23, 25–26, 28–30, 32, 34, 37, 39–79, 85–103, 121–146, 176–193, 195, and 207–209) still have rich spectral contents covering the visible, near-infrared, and shortwave infrared spectral regions. This is sufficient for this study.
2) Georeference
   The original hyperspectral imagery delivered by JPL need to be georeferenced. An image to image rectification was adopted in this step by using the USGS DOQs generated from NAPP 1999 CIR aerial photography. All DOQs are referenced to the North American Datum of 1983 (NAD 83) and cast on the Universal Transverse Mercator (UTM) projection. The accuracy and quality of USGS DOQs meet NMAS at 1:12,000 scale for 3.75-minute quarter quadrangles and at 1:24,000 scale for 7.5-minute quadrangles.

Table 1
Sample size for each class used in this study.

Class #	Vegetation type	Size	Class #	Vegetation type	Size
1	Dry Prairie	260	9	Melaleuca	108
2	Improved Pastures	256	10	Hardwood/Coniferous Mix	250
3	Groves	180	11	Mangrove Swamp	260
4	Fruit Orchards	164	12	Mixed Wetland Hardwoods	104
5	Upland Shrub and Brush	146	13	Mixed Shrubs	154
6	Pine Flatwood	326	14	Cypress	62
7	Upland Hardwood Forest	180	15	Freshwater Marshes	64
8	Brazilian Pepper	66	Total: 2580		

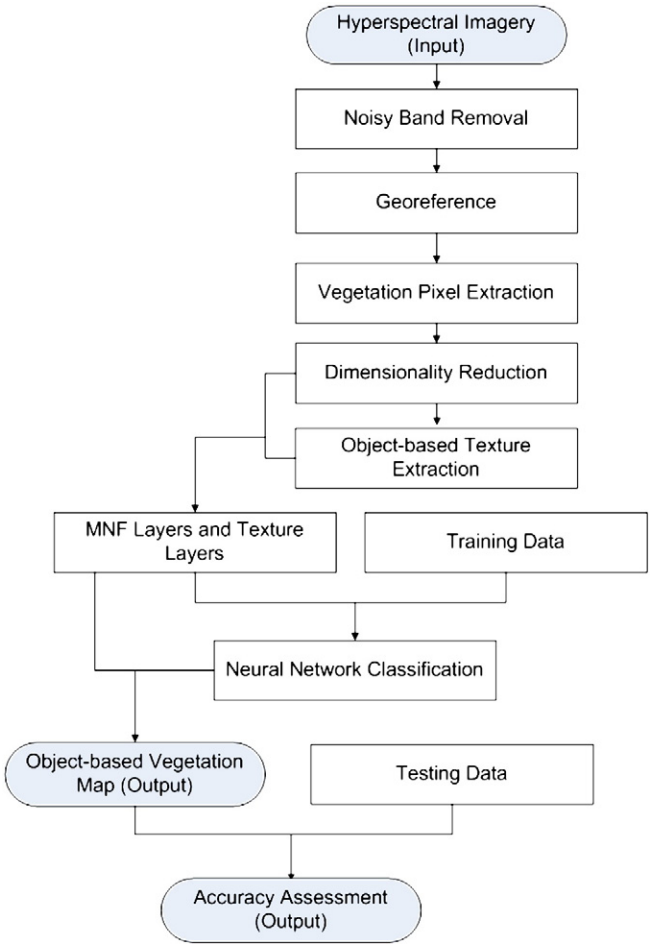

Fig. 2. Flowchart of vegetation mapping in the Everglades from hyperspectral imagery.

The DOQs were also employed by the SFWMD to compile the reference data. By this way, the imagery was geographically aligned with the reference data.

3) Vegetation pixel extraction
As shown in Fig. 1, non-vegetation features were also presented in the selected area, which are not of interest in this study and were masked out for further analysis. The Normalized Difference Vegetation Index (NDVI) can be used to differentiate vegetation and non-vegetation features. Generally, for hyperspectral imagery, reflectance from a red channel centered on 660 nm and a near-infrared channel centered on 860 nm are used to calculate the NDVI (Jensen, 2005). We derived a NDVI layer from the hyperspectral data and then built a vegetation mask by applying a NDVI threshold. The optimal NDVI threshold was determined by visual examinations of several tests with different thresholds. Non-vegetation pixels will not be processed, which can reduce the computational cost in the further steps.

4) Dimensionality reduction
Hyperspectral data contain a tremendous amount of redundant spectral information. Statistical analysis reveals that many of the bands are highly correlated. The commonly used approach, Minimum Noise Fraction (MNF) transformation (Green et al., 1988) was used to reduce the high dimensionality of the data and computation requirements of further processing. The MNF transformation applies two cascaded principal component analyses, with the first transformation decorrelating and rescaling noise in the data, and the second transformation creating coherent eigenimages that contain useful information, and generating noise-dominated eigenimages. The transformation generates the eigenvalues and corresponding eigenimages, both of which are used to determine the true dimensionality of the data. Useful MNF eigenimages typically have an eigenvalue an order of magnitude greater than those that contain mostly noise. We conducted the MNF transformation in ENVI 4.7. A plot of eigenvalues against the output MNF layers was generated. A due inspection of this plot and visual inspection of the eigenimages revealed that 15 MNF layers should be selected for this study.

5) Object-based texture information extraction
Texture analysis generates a spatial variability measure that can be integrated with spectral data in the classification methods. Researchers often adopt the kernel-based texture analysis methods which utilize a single square moving window over which to calculate texture measures for each pixel. One challenge in these methods is the determination of optimal kernel size. A large window can produce a stable texture measure, but generates large edge effects. A small window can minimize edge effects, but often does not provide stable texture measures (Ferro & Warner, 2002). The object-based texture analysis, i.e. deriving texture information on the object level, is more reasonable because it calculates the texture measures in an adaptive window with variable size and shape. The object-based image analysis offers the capability for identifying regions of varying shapes and sizes in an image, which can be used for subsequent texture extraction (Blaschke, 2010). We thus derived the texture measures on the object level. The multiresolution segmentation algorithm in eCognition Developer 8.64.1 was used to generate the image objects. This algorithm starts with one-pixel image segments, and merges neighboring segments together until a heterogeneity threshold is reached (Benz et al., 2004). The heterogeneity threshold is determined by a user-defined scale parameter, as well as color/shape and smoothness/compactness weights. The image segmentation is scale-dependent, and the quality of segmentation and overall object-based classification are largely dependent on the scale of the segmentation (Liu & Xia, 2010). In order to find an optimal scale for image segmentation, an unsupervised image segmentation evaluation approach (Johnson & Xie, 2011) was used. This approach conducts a series of segmentations using different scale parameters first, and then identifies the optimal image segmentation using an unsupervised evaluation method that takes into account global intra-segment and inter-segment heterogeneity measures. A global score can be generated for each segmentation result. This global score combines the normalized weighted variance and Moran's *I* value. It can be used to determine the optimal scale for the segmentation. For our study area, a series of segmentations was carried out using 10 different scale parameters (2–20 at an interval of 2). Preliminary analyses revealed that scale parameter larger than 20 generated more under-segmented objects and smaller than 2 produced more over-segmented objects. For this reason, segmentation results from scale parameters smaller than 2 or large than 20 were not evaluated. The global score for each segmentation was calculated and then the best segmentation with the lowest global score was selected. The first five MNF layers were set equal weights with a value of 5 and the last 10 MNF layers were set equal weights with a value of 1. This specification was based on the eigenvalues of each MNF layer produced. Color/shape weights were set to 0.9/1.0 so that spectral information would be considered most heavily for segmentation. Smoothness/compactness weights were set to 0.5/0.5 so as to not favor either compact or non-compact segments. The segmentation procedure was conducted using eCognition Developer 8.64.1.
Other challenges in texture analysis include the selection of texture order, measures, and spectral bands. The review of texture research by Warner (2011) concludes these selections are case- and class-specific. For this study, the first-order and second-order texture metrics were tested because the third or higher order texture

information lacks the theoretical justification. First order texture measures are statistics calculated from the original image values and do not consider pixel neighbor relationships. Second order texture measures consider the relationship between groups of two pixels in the original image. Hall-Beyer (2007) suggests choosing one of the contrast measures (contrast, dissimilarity, and homogeneity), one of the orderliness measures (angular second moment, maximum probability, and entropy), and two or three descriptive statistics measures (mean, variance, and correlation) metrics, because many texture measures are intrinsically similar. For this study, we tested a combination of one of the contrast measures (i.e. homogeneity), one of the orderliness measures (i.e. entropy), and two of the descriptive statistics measures (i.e. mean and variance) as the second-order metrics in the classification. The grey level co-occurrence matrix (GLCM) algorithm in eCognition was used to extract the object-based second-order texture measures. The directionally invariant texture measures were produced by calculating the mean of the texture results in all four directions (0°, 45°, 90°, and 135°). The calculation of GLCM texture measures in eCognition is independent of the image data's bit-depth. The software can dynamically interpolate the input data to 8 bit before evaluating the co-occurrence. All image object pixels are scanned and employed in the GLCM calculation. To reduce the object border effects, pixels bordering the segments directly (surrounding pixels with a distance of 1) are additionally taken into account in the calculation (Trimble, 2011). For comparison purpose, the mean, variance, and entropy were selected as the first-order texture metrics and calculated in eCognition at the object level. These texture measures were only calculated for the first three MNF layers because they contain most of the information in the original hyperspectral data. Finally, three additional images were produced. The first one integrated 15 MNF layers and 9 first-order texture layers, and the second one combined 15 MNF layers with 12 second-order texture layers, and the third one combined 15 MNF layers with 9 first-order and 12 second-order texture layers. These images will be explored for vegetation mapping in further steps.

6) Neural network classification

Neural network is inspired by the structure of the neurons and synapses of human brains. The commonly used neural networks in remote sensing include multi-layer perceptron (MLP), radial-basis function (RBF), adaptive resonance theory (ART), and self-organizing map (SOM). For hyperspectral image processing, the learning vector quantization (LVQ) neural network classifier (i.e. supervised SOM) (Kohonen et al., 1996) is desirable due to its relatively simple structure and less parameters to be specified. However, the original LVQ method may not achieve expected accuracy for complex wetland vegetation discrimination because it assumes each class has the same number of spectral representatives (i.e. codebooks). This may lead to overestimation or underestimation of the number of signatures for some classes, thus will inevitably have negative impacts on the final classification accuracy (Zhang & Qiu, accepted for publication). The Everglades has a very complicated plant community with diverse types, varying ages and growing conditions, and high spatial heterogeneity. These factors combined result in a high degree of between-class spectral and spatial confusion and a great deal of within-class spectral and spatial variability. Multiple signatures often appear for one vegetation type in this complex environment. It is thus necessary to improve the LVQ so that the between-class spectral and spatial confusion and within-class spectral and spatial variability can be modeled, as well as the true number of signatures for each class can be characterized. A variety of modifications of LVQ were reported in the literature to ensure faster convergence, a better adaption of the receptive fields to optimum Bayesian decision, or an adaptation for complex input data structure (Villmann et al., 2003). However, an adaption of the competitive neurons with an attempt to obtain the true number of signatures within a class was not reported. We therefore developed an Adaptive LVQ (ALVQ) neural network for vegetation classification in the Everglades. The topological structures of original LVQ without hidden layers and the ALVQ are shown in Fig. 3.

Unlike the LVQ that is unable to well model the multiple signatures within a class (Fig. 3A), the ALVQ has three layers: an input layer, a competitive layer, and an output layer (Fig. 3B). The neurons in the

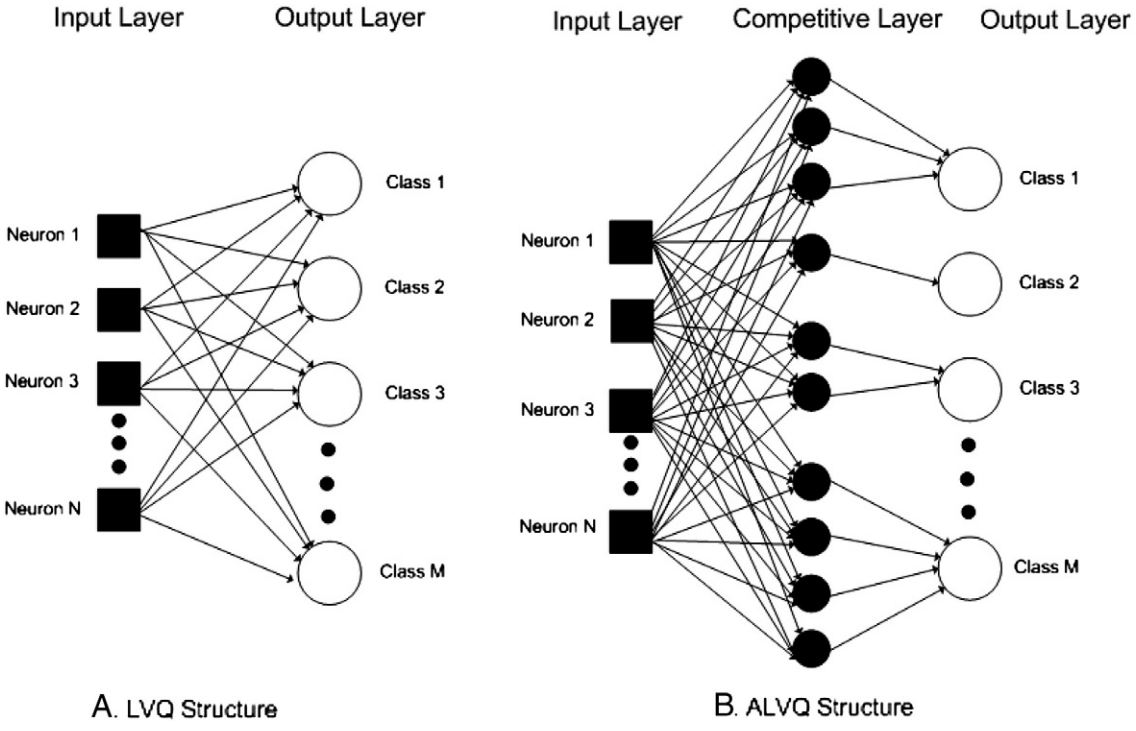

Fig. 3. Topological structures of LVQ (A) and ALVQ (B).

input layer correspond to the digital values of input data. The number of input neurons (i.e. N) equals the number of layers or bands of the input imagery. The number of neurons in the output layer equals the number of vegetation types (i.e. M). The number of neurons in the competitive layer can be equal to or greater than that of the output classes. When the number of competitive neurons is more than the number of output classes, each class is allowed to have multiple clusters so that the modeling of possible multimodal distributions in the data is possible. The ALVQ classifier can automatically adapt the number of neurons in the competitive layer based on a Student t-test. Externally the ALVQ is a supervised system, but internally, it has a fully unsupervised engine that can generate an appropriate number of competitive neurons for each output class. The output and competitive layers are not fully connected, as shown in the illustration. The ALVQ consists of four components: 1) unsupervised clustering, 2) supervised learning, 3) determination of number of competitive neurons, and 4) object-based vegetation classification. Each component is described in detail below.

Unsupervised clustering: To effectively model the characteristics of multiple signatures within each vegetation type, internally unsupervised SOM clustering for each class is performed first with a predetermined number of clusters (e.g. 5). SOM is often used to group inputs into different categories with the 'winner-take-all' strategy. In the ALVQ algorithm, a winner whose weight has the minimum distance from the input vector will be determined first, and then the network updates the weight of this winner via a learning rule. In this way, the competitive neurons become selectively tuned to the input patterns presented during this competitive-learning procedure. In this study, for a pixel with N layers as an input vector $(x_1, x_2, \ldots x_N)$, the winner output neuron is decided by:

$$\min\left(\left\|x_i - c_{ij}\right\|\right) \quad (j = 1, 2, \ldots L) \tag{1}$$

where c_{ij} is the weight linking the ith layer input and jth cluster of an output class. c_{ij} is also known as the codebooks, prototypes, and mean in the literature. N is the dimensionality of x, L is the total number of clusters for each class, and $\|*\|$ is any norm expressing the similarity between an input vector and the weights. For this study, the similarity is determined by Euclidean distance.

Supervised learning: The weight (c_{ij}) which represents the signatures of each class is updated during the training process by using the externally supervised learning algorithm, which is, utilizing the true vegetation type information provided by the training data. The updating scheme is:

$$\Delta c_{ij} = \eta\left(x_i - c_{ij}\right) \text{if neuron } j \text{ is the winner} \tag{2}$$

$$\Delta c_{ij} = 0, \text{otherwise} \tag{3}$$

where η is the learning rate. The winner is determined through within-class competition instead of between-class competition. The vegetation type is informed by the training data. Note that the LVQ algorithm and many modifications push c_{ij} away from the unmatched (incorrectly classified) input pattern, ALVQ uses only one learning scheme for the mean parameter because of the high degree of similarity of spectral characteristics between vegetation types. The "pushing away" scheme may push the mean parameter far from the center of the cluster, resulting in unexpected learning results.

Determination of number of competitive neurons: After the unsupervised clustering and supervised learning, the input training data for each class will be grouped into clusters. To generate the true number of signatures for each class, a two sample Student t-test is used to assess the similarity of two adjacent clusters. The two-sample Student t-test can test the equality of two means from two groups with equal sample sizes and equal variance, or with unequal sample sizes and equal variance, or with unequal sample sizes and unequal variance. After the unsupervised clustering, clusters within each class should have different sample size and variance. Thus the two-sample t-test for unequal sample sizes and unequal variance was used with the equations as:

$$t = \frac{c_{ij} - c_{(i+1)j}}{s_{c_{ij} - c_{(i+1)j}}} \tag{4}$$

$$s_{c_{ij} - c_{(i+1)j}} = \sqrt{\frac{\sigma_{ij}^2}{n_1} + \frac{\sigma_{(i+1)j}^2}{n_2}} \tag{5}$$

where c_{ij} is the same parameters as for Eq. (1), and n_1 and n_2 are the total number of samples for cluster i and cluster $i+1$, respectively. σ_{ij} is the standard deviation of ith layer input for the jth cluster. A p value for each test can be calculated based on the t distribution. If the p value is greater than 0.05, indicating the two clusters are not statistically different, then the two adjacent clusters are merged; otherwise, they are kept separated. The merging of the clusters can be conducted iteratively until no more merging is needed. In this way, the number of competitive neurons for each vegetation type can be finally determined automatically.

Object-based vegetation classification: All the automatically generated codebooks from the internally unsupervised clustering and externally supervised learning can be used to directly classify the data. For this study, an object-based classification was conducted according to the nearest neighbor rule. A mean profile of the input data for a segmented object is calculated first, and then this mean profile comes into the system as an input vector. This segmented object will be assigned to a vegetation type whose codebook has the minimum distance to this input vector. The ALVQ algorithm was implemented using Visual Basic.NET programming language under Microsoft Visual Studio 2010 developing environment.

7) Accuracy assessment

It is necessary to assess the accuracy of the finally generated object-based vegetation map. The conventional error matrix and Kappa statistics approaches in remote sensing (Jensen, 2005) were used to evaluate the performance of the developed procedure and the derived vegetation map.

3.2. Experimental analyses

To obtain an effective and accurate procedure for vegetation classification in Everglades, a number of tests were conducted. We first designed two experiments to examine the impact of the MNF transformation on vegetation discrimination. The first experiment (hereafter Experiment 1) used the original hyperspectral data with noisy bands eliminated (i.e. $N = 127$), and the second experiment (hereafter Experiment 2) used the MNF transformed imagery with 15 MNF layers selected (i.e. $N = 15$). To assess the usefulness of the object-based texture information in vegetation discrimination, we designed another three experiments, leading to experiments 3, 4 and 5. Experiment 3 combined the first-order texture measures, experiment 4 combined the second-order texture measures, and experiment 5 combined both first-order and second-order measures with the MNF layers as inputs in ALVQ respectively. To evaluate the performance of the ALVQ, three conventional classifiers, minimum distance method, spectral angle mapper (SAM) approach, and maximum

likelihood (ML) technique were applied in the classification. The LVQ neural network method without hidden layers and another machine learning based technique, support vector machines (SVMs), were also tested for comparison. The literature has shown that the SVMs are promising methods in hyperspectral image analysis. The aim of SVMs is to find a hyperplane that can separate the input dataset into a discrete predefined number of classes in a fashion consistent with the training samples. Detailed descriptions of SVM algorithms are given by Huang et al. (2002) and Melgani and Bruzzone (2004) in the context of remote sensing. Kernel based SVMs are commonly used for remote sensing image classification, among which the radial basis function (RBF) kernel and the polynomial kernel are frequently employed. For the RBF kernel method, the penalty error parameter (C) and kernel width (γ) need to be defined. The polynomial kernel method needs to define the degree parameter (p). For this study, both methods were examined and the one producing the best accuracy was compared with the ALVQ result. Similar to experiment 5, first-order and second-order texture measures were combined with the MNF layers and then classified by these methods.

4. Results

4.1. Experiment results

The performance of different experiments was evaluated based on the error matrix whose information can be summarized as an overall accuracy and Kappa value. The overall accuracy is defined as the ratio of the number of validations pixels that are classified correctly to the total number of validation pixels irrespective of the class. The Kappa value describes the proportion of correctly classified validation pixels after random agreement are removed. Most researchers generated these two measures with a one-time running of the selected algorithms. The reported values of the accuracy measures may be biased if different training and testing data are utilized. For this study, we ran each experiment and testing classifiers many times with an attempt to produce robust accuracy measures. For each running, reference data (i.e. 2580 samples) were randomly split into 50% for training and 50% for testing with a constraint of ensuring no overlapping between the training and testing data. The procedure will not terminate until a stable averaged overall accuracy and Kappa value were obtained. This is similar to the commonly used Monte Carlo experiment in statistics.

The generated overall accuracies and Kappa values from experiments 1 and 2 are displayed in Table 2. The application of all spectral bands (i.e. 127 bands) produced a lower accuracy. The MNF technique increased the overall accuracy from 55% with a Kappa value of 0.52 to 86% with a Kappa value of 0.84 (Table 2). To examine the significance of the result, the Kappa z-score statistical test based on the error matrix was conducted. The derived values of z-score for experiments 1, and 2 are 34.56 and 79.60 respectively (Table 2), which suggests both experiments are significantly better than a random classification at the 95% statistical confidence level. Kappa techniques are also often used to test the statistical difference between results. A z-score value of 18.19 was obtained based on the error matrix generated from experiments 1, and 2. The Kappa test assumes the samples used in the calculation are independent, an assumption that was unsatisfied in most studies because the samples were related. The McNemar test (Foody, 2004) is one of alternatives to evaluate the statistical significance of differences in accuracy for related samples. This test is based upon a confusion matrix (2 by 2 in dimension) generated from two classifications and the reference data. The result from McNemar test for experiments 1 and 2 is displayed in Table 2. A z-score value of 21.9 was generated, indicating that experiment 2 generated significantly better outcomes than experiment 1. This was confirmed by both Kappa and McNemar tests.

Table 2
Classification accuracies and statistical tests from five designed experiments in ALVQ.

Accuracy and Kappa statistics for each experiment			
Experiment #	Overall accuracy	Kappa value	z-score
1	55%	0.52	34.56*
2	86%	0.84	79.60*
3	90%	0.89	99.73*
4	92%	0.91	111.52*
5	94%	0.94	135.37*
Pairwise statistical test			
Experiment	Kappa (z-score)		McNemar (z-score)
1/2	18.19*		21.9*
2/3	3.59*		3.0*
2/4	5.16*		5.8*
3/4	1.60		0.6
3/5	4.01*		2.2*
4/5	2.43*		3.4*

Notes:
Experiment 1: original hyperspectral data with 127 bands.
Experiment 2: MNF data with 15 layers.
Experiment 3: first-order texture layers and 15 MNF layers.
Experiment 4: second-order texture layers and 15 MNF layers.
Experiment 5: first-order and second-order texture layers and 15 MNF layers.
The critical value of z-score is 1.96 at a confidence level of 0.95.
* : significant with 95% confidence.

Similarly, after running experiments 3, 4, and 5 many times using the ALVQ, the averaged overall accuracy and Kappa statistics are generated and displayed in Table 2. Combination of the texture information with the MNF transformed image largely improved the classification result. The first-order texture measures increased the overall accuracy to 90% with a Kappa value of 0.89. Better accuracy was achieved by combining the second-order texture measures, which had an overall accuracy of 92% and a Kappa value of 0.91. The best accuracy was achieved by combining both first-order and second-order texture measures with the MNF layers, which generated an overall averaged accuracy of 94%, and a Kappa value of 0.94. Similarly, the Kappa statistical tests were carried out for the outcome from each single experiment first, and then results between experiments. The tests reveal that all the experiments generated significantly better results than a random classification, with values of z-score of 99.73, 111.52, and 135.37 respectively. The Kappa and McNemar tests of between-experiment outcomes illustrated that object-based texture measures significantly improved the accuracy, with the second-order measures contributing more in classification; there was no significant difference between first-order measures and second-order measures in this case; combination of both first-order and second-order measures to the MNF layers generated significantly better results than combining any single order measures. Further tests for each texture measure reveal that the selected three measures at the first order had similar contributions to the classification. For GLCM texture measures, the mean and variance contributed more than the homogeneity and entropy in classification. The GLCM mean and variance had similar contributions, and the GLCM homogeneity and entropy had similar contributions.

4.2. Performance of different classifiers

The performance of classifiers was also evaluated using overall accuracies and Kappa values. The minimum distance, SAM, maximum likelihood, and SVM algorithms have been integrated into ENVI 4.7 that is written using the Interactive Data Language (IDL) programming language. Multiple implementations of these algorithms can be achieved under IDL. Similarly, we ran these algorithms many times with random training and testing data selected for each running. The classification accuracies and Kappa statistics from these methods are listed in Table 3. The minimum distance, SAM, and LVQ

classifiers generated same overall accuracies (75%) and Kappa values (0.73) with slightly different *z*-score values. The maximum likelihood (ML) method presented a poor result with an overall accuracy of 67% and Kappa value of 0.65. The SVM produced a better result with an overall accuracy of 88% and Kappa value of 0.86. Kappa statistical tests illustrate that the results from these methods are significantly better than a random classification at a confidence level of 0.95. Comparison of the outcomes from these methods with the result listed in Table 2 from ALVQ (i.e. experiment 5) illustrated that the ALVQ achieved the best accuracy in this case. The Kappa and McNemar statistical tests for the between-classifier performance indicate that the ALVQ generated significantly better result than the traditional classifiers and the LVQ neural network, as supported by the higher *z*-score values listed in Table 3. The McNemar test, however, indicates the ALVQ was not significantly different from the SVM in classification.

Researches of neural networks in remote sensing illustrated that some neural networks such as the most commonly used MLP are sensitive to the size of training set (Atkinson & Tatnall, 1997). To examine the sensitivity of ALVQ to the size of training data, a series of implementations of ALVQ were conducted using different size of training data. We first randomly selected 20% of the reference data as a separate testing dataset, and then changed training sample sizes from the remaining reference data (10%–70% at an interval of 10%) for running ALVQ. Again, for each implementation, we ran the ALVQ many times to generate an averaged overall accuracy and Kappa value. Note that the selected testing data were not changed for each running and implementation to ensure an unbiased assessment. The results from these tests are displayed in Table 4. It suggests that the ALVQ is not sensitive to the size of training data. Similar overall accuracies and Kappa values were produced using different training samples. For our case, the overall accuracy and Kappa values became stable when 40% or more training data were selected.

4.3. Object-based vegetation mapping

From the above two subsections, we can see that experiment 5 which combined first-order and second-order texture measures with the selected MNF layers as the input neurons in the ALVQ produced the best accuracy. Thus, the final spatial and spectral codebooks learned from experiment 5 were used to generate the object-based vegetation map in our study area, as shown in Fig. 4. The vegetation map at the object level is more informative and useful than a traditional pixel-based one which may be noisy due to the high degree of spatial and spectral heterogeneity of the Everglades. The derived error matrix and corresponding producer's and user's accuracy for each type from experiment 5 are listed in Table 5. The producer's accuracy varies from 74% to 100%, and the user's accuracy ranges from 78% to 100% for different vegetation type. Hardwood/Coniferous mix (class 10) and mixed wetland hardwoods (class 12) have a relatively lower accuracy due to the spatial and spectral complexity caused by the mixture of different hardwoods. An accuracy of 100% was achieved for mangrove swamp discrimination, which is encouraging because they play critical roles in supporting a variety of habitats in the Everglades. Good accuracies was also obtained for two invasive exotic species, Brazilian Pepper (class 8), and Melaleuca (class 9). Accurate identification of invasive exotic species in south Florida is critical because tremendous time, effort, and expense are required for their discrimination, eradication, and control in the Everglades. The use of hyperspectral data provides the great potential to detect these exotic species.

Table 3
Classification accuracies from other fiver classifiers.

Classifier	Overall accuracy	Kappa value	z-score
Minimum distance	75%	0.73	56.26*
SAM	75%	0.73	56.43*
LVQ	75%	0.73	55.95*
ML	67%	0.65	47.05*
SVM	88%	0.86	86.73*
Pairwise statistical test			
Classifier	Kappa (*z*-score)	McNemar (*z*-score)	
Minimum distance/ALVQ	14.16*	9.4*	
SAM/ALVQ	13.89*	9.3*	
ML/ALVQ	18.92*	14.2*	
SVM/ALVQ	6.14*	1.8	
LVQ/ALVQ	14.26*	15.5*	

Notes:
SAM: spectral angle mapper
ML: maximum likelihood
SVM: support vector machine
LVQ: learning vector quantization
ALVQ: adaptive learning vector quantization
The critical value of *z*-score is 1.96 at a confidence level of 0.95.
* : significant with 95% confidence.

5. Discussions

5.1. MNF transformation

Many researches in hyperspectral applications for vegetation mapping used the MNF transformation to determine the endmembers of the vegetation covers and conducted the classification from the original spectral bands (e.g., Artigas & Yang, 2005; Rosso et al., 2005). The endmember-based algorithms are commonly dependent of a spectral library that was built from the original measured spectrum. It is difficult to evaluate the impact of the inherent noise in hyperspectral data on final classification using the endmember-based methods because it is complicated to implement MNF transformation to the spectral library. Several researchers have found that the MNF transformed hyperspectral imagery is more effective in vegetation mapping (e.g. Belluco et al., 2006; Yang et al., 2009). The result from this study confirms these findings. The MNF transformation not only helps reduce the dimensionality of hyperspectral data to save the computational cost, but also largely improves the classification accuracy. This may be attributed to the fact that the MNF technique is capable of minimizing the inherent noise in the image. Thus, it is suggested that the MNF transformation is not only necessary, but also important for vegetation mapping in the Everglades from the hyperspectral data.

5.2. Classification techniques

The study illustrates that the proposed ALVQ is an effective classifier for vegetation mapping in complex wetland environments. The minimum distance, SAM, and LVQ all assume a single signature for each class. The minimum distance method takes the mean profile of a class from the training data as the signature for this class, while the SAM uses the endmember as the signature, and the LVQ employs the finally trained codebook (i.e. the weight) as the signature. These three methods generated fair accuracies because of the high degree of heterogeneity in the Everglades. The maximum likelihood (ML) algorithm requires the spectral response of each class displays a

Table 4
Overall accuracies and Kappa values generated from ALVQ using different size of training data.

Training data	Overall accuracy	Kappa value
10%	90%	0.89
20%	92%	0.91
30%	93%	0.92
40%	94%	0.94
50%	94%	0.94
60%	94%	0.94
70%	94%	0.94

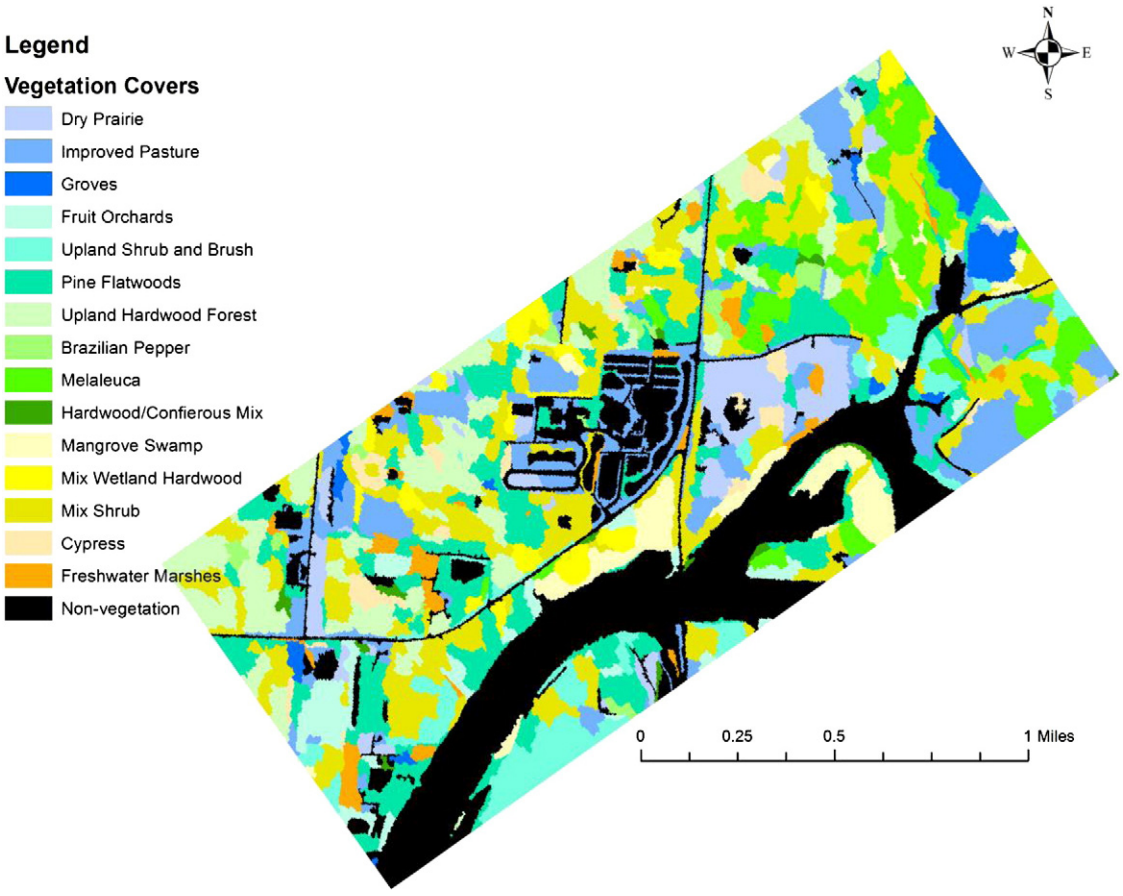

Fig. 4. Object-based vegetation map for the study area.

Gaussian distribution. Several hyperspectral studies in vegetation mapping have found that ML produced better accuracy than other traditional methods (*e.g.*, Belluco et al., 2006; Jollineau & Howarth, 2008; Yang et al., 2009). However, in our study, the ML produced a poor result, which may be caused by the adoption of a combination of spectral and spatial features in the classification. This integration can hardly guarantee the Gaussian distribution of the data.

The support vector machine (SVM) algorithm is a promising methodology in hyperspectral image analysis. In recent years there has been a significant increase in SVM works on remote sensing problems. A recent review of SVMs by Mountrakis et al. (2010) reported that a key advantage of SVMs compared with other classifiers is that they can achieve better results when a limited amount of reference data available. A major setback concerning the practice of SVMs for

Table 5
Error matrix for the classification from experiment 5 using ALVQ.

Class	1	2	3	4	5	6	7	8	9	10	11	12	13	14	15	Row total	PA (%)	UA (%)
1	125		2						3							130	96	98
2	2	126														128	98	100
3			90													90	100	98
4				77						1		4				82	94	100
5					72								1			73	98	96
6						152	4		2	1		1	3			163	93	96
7					3		86	1								90	96	83
8								33								33	100	80
9									54							54	100	90.
10						6	8	6		93		7	5			125	74	96
11											130					130	100	100.
12						1	3	1				47				52	90	78
13							3		1			1	72			77	94	87
14										1				30		31	97	100
15													1		31	32	97	100
Col. Total	127	126	92	77	75	159	104	41	60	96	130	60	82	30	31	1290		

Total accuracy: 94%
Kappa value: 0.94
PA: producer's accuracy
UA: user's accuracy
The column is the reference data, and the row is the classification data

remote sensing image classification is the choice of kernels and the setting of other parameters, which can substantially affect the classification accuracy (Yang, 2011). For this study, the optimal setting of C and γ in the RBF kernel SVM algorithm was determined by a grid search strategy that tests possible combinations of C and γ in a user-defined range. The optimal setting of the degree parameter (p) in the polynomial kernel SVM algorithm was determined by a series of tests using different p values in terms of accuracy. Testing results reveal that the polynomial kernel is more suitable for our dataset and the best accuracy from this method is displayed in Table 3. The SVM obtained a comparable accuracy with the ALVQ. The high spatial resolution of the data permits the on-screen collection of a large number of reference pixels for classifier training, thus the advantage of the SVMs may not be clear for this scenario. Among these methods, the ALVQ achieved the best accuracy in discriminating 15 vegetation types in this study. This may be attributed to its capability to model the multiple spectral and spatial signatures within each class through the built-in unsupervised clustering, as well as its power to characterize the spectral and spatial differences between classes. The adaptability of the competitive layer in ALVQ and the learning scheme used the ALVQ excluding the "pushing away" strategy are also helpful for the achieved results.

Qiu and Jensen (2004) developed a neuro-fuzzy system by modifying the LVQ to model the multiple within-class spectral signatures and applied it to hyperspectral image classification after further improvements (Qiu, 2008). Similar to the original LVQ approach, one setbacks of this neuro-fuzzy system is that it assumes each class has the same number of spectral representatives, which will inevitably have negative impacts on the final classification accuracy. To address this issue, Zhang & Qiu (accepted for publication) improved the algorithm and developed an Adaptive Gaussian Fuzzy Learning Vector Quantization (AGFLVQ) classifier that can automatically determine the number of within-class signatures. An application of AGFLVQ achieved a reasonable accuracy to identify urban tree species from hyperspectral imagery. However, one of the limitations of both the original and improved neuro-fuzzy classifiers is that the system will become unstable if only one signature exists for a class. This is because the standard deviation parameter that models the within-class data dispersion may become a small number (close to zero) in the learning step if the training data for this class have very similar spectral profiles. The small number will lead to a crash of the system since this parameter appears as a denominator in the adopted Gaussian function. Elimination of the Gaussian fuzzification idea from the algorithms should make them more operational and robust in practice. This is confirmed by this study. Exclusion of the Gaussian fuzzification can also reduce the computational cost in classification.

5.3. Potential contribution of hyperspectral technology to the Everglades

Mapping vegetation types in the Everglades is a challenge in remote sensing due to its high spatial and spectral heterogeneity and rich vegetation types. A number of efforts were undertaken to produce vegetation maps for subareas of the Everglades from air photos or very high spatial resolution satellite data (Jones, 2011). To provide baseline vegetation composition data for CERP, a hybrid approach relying on visual interpretation of color infrared photography through analytical stereo plotters has been developed (Rutchey et al., 2008). With the emergence of hyperspectral remote sensing data, it has been anticipated that the generation of vegetation maps with adequate accuracy can be automated. This is particularly urgent for the current CERP. But exploitation of increased spectral data for plant study in the Everglades environment is not simple. Hirano et al. (2003) reported a moderate accuracy (i.e. 66% correct) for vegetation mapping over the southern end of the Everglades National Park. This moderate accuracy was caused by the inadequate spatial resolution of their adopted hyperspectral data (i.e. 20 m) and their limited examination of data transformation and classification techniques. They only examined the SAM method and did not test any advanced approaches which are capable of characterizing the within-class features. For our study, we obtained an overall classification accuracy of more than 90%. This is believed to be a result of the high spatial and spectral resolution of the data, the effectiveness of the ALVQ, the adoption of data transformation, plus the combination of useful texture information in the classification. Belluco et al. (2006) have indicated that the use of high spatial resolution dataset for vegetation mapping is particularly advantageous in heterogeneous wetland environments where such datasets can reduce within-pixel heterogeneity, thereby increasing spectral separability. In addition, fine spatial resolution permits the collection of a large number of reference pixels for classifier training, which can improve the classification. Data transformation is important in hyperspectral applications. Although hyperspectral techniques provide rich spectral contents that largely enhance their power in material identification, the redundant bands and inherent noises in the data, on the other hand, may severely reduce their capability. Determination of the true dimension of the data to make a balance of these two sides is important in their applications. The selection of classification algorithms in the Everglades is also very important. The relatively simple classifiers may not generate an expected accuracy, especially for regions with very high spatial heterogeneity. Advanced approaches such as neural networks or machine learning techniques are more attractive to characterize vegetation in the Everglades. Texture information is critical in vegetation classification, especially for analyzing fine spatial resolution data. Some vegetation covers may have similar spectral contents but different textures. Combination of texture measures may significantly improve the mapping results.

The study indicates that fine spatial resolution hyperspectral data is promising to replace the current air photo based vegetation mapping to support CERP. The potential application of hyperspectral data in the Greater Everglades could be quite significant if implemented in an appropriate manner. One key aspects of hyperspectral technology is that the data collected can be dissected and reassembled in many different ways, thus allowing the same data collection effort to be used to answer different questions. While one project may be interested in exotic vegetation spread and control, and the other project is concerned the impacts of restoration on community structure, hyperspectral data collected from the same flight can be used to address both questions at the same time or on different dates. This allows both the concepts of economy of scale and funds leveraging to be applied, thus significantly reducing the cost. Hyperspectral technology can not only benefit the on-going CERP, but also help with the management of entire South Florida.

6. Conclusions

The purpose of this study is to explore the potential of fine spatial resolution hyperspectral imagery for vegetation mapping in the Greater Everglades. To generate an informative and accurate vegetation map, we designed an automated procedure that combines four remote sensing fields: object-based image analysis, texture analysis, neural networks, and hyperspectral technology. The results derived from this study indicate that a combination of these four techniques is powerful for vegetation mapping in the Everglades. The study illustrates that the developed Adaptive Learning Vector Quantization (ALVQ) is able to accurately classify vegetation because of its capability in characterizing the within-class spatial and spectral variation and modeling the between-class spatial and spectral confusion. The ALVQ is also efficient in processing hyperspectral data due to its relatively simple structure and straightforward learning scheme. Combining spatial information in the form of object-based texture measures with the developed neural network can significantly improve the classification accuracy. This suggests that the spatial features in fine spatial resolution imagery are very useful in vegetation

discrimination. We also find that the MNF transformation not only can reduce the data dimensionality, but also improve the classification. There is no significant difference in classification between the first-order texture measures and the second-order texture measures in this study, but a combination of both with the MNF layers as the input units in the ALVQ achieved the best accuracy. An object-based vegetation map was obtained with an overall accuracy of 94% and Kappa value of 0.94. Such a high accuracy is believed to be a result of the high spatial and spectral resolution of the data, effective data transformation, adoption of the developed ALVQ, as well as the combination of spatial information in the classification.

The designed procedure and developed algorithm for automatically processing fine spatial resolution hyperspectral imagery in wetland vegetation mapping achieved good result in the testing study area. Considerable additional work is needed in other wetland areas with different vegetation community and species in order to examine the robustness and extensibility of this procedure. It is also informative to compare the object-based texture analysis with the kernel-based texture analysis to test the performance of these two methods in vegetation mapping. The contribution of each texture measure and different combination of these measures also needs to be examined. These are major dedications in the future study. It is anticipated that this study can benefit global wetland mapping in general, and the Greater Everglades in particular.

Acknowledgements

The authors appreciate the constructive comments and suggests from two anonymous reviewers to improve this paper.

References

Adam, E., Mutanga, O., & Rugege, D. (2010). Multispectral and hyperspectral remote sensing for identification and mapping of wetland vegetation: A review. *Wetlands Ecology and Management*, *18*, 281–296.

Artigas, F. J., & Yang, J. S. (2005). Hyperspectral remote sensing of marsh species and plant vigour gradient in the New Jersey Meadowlands. *International Journal of Remote Sensing*, *26*, 5209–5220.

Atkinson, P. M., & Tatnall, A. R. L. (1997). Introduction neural networks in remote sensing. *International Journal of Remote Sensing*, *18*, 699–709.

Batista, M. H., & Haertel, V. (2010). On the classification of remote sensing high spatial resolution image data. *International Journal of Remote Sensing*, *31*, 5533–5548.

Belluco, E., Camuffo, M., Ferrari, S., Modenese, L., Silvestri, S., Marani, A., et al. (2006). Mapping salt-marsh vegetation by multispectral and hyperspectral remote sensing. *Remote Sensing of Environment*, *105*, 54–67.

Benz, U., Hofmann, P., Willhauck, G., Lingenfelder, I., & Heynen, M. (2004). Multi-resolution, object-oriented fuzzy analysis of remote sensing data for GIS-ready information. *ISPRS Journal of Photogrammetry and Remote Sensing*, *58*, 239–258.

Blaschke, T. (2010). Object based image analysis for remote sensing. *ISPRS Journal of Photogrammetry and Remote Sensing*, *65*, 2–16.

Campbell, J. B. (1996). *Introduction to remote sensing.* New York: The Guilford Press.

Comprehensive Everglades Restoration Plan (CERP). Accessed on 12 April 2012 from. , http://www.evergladesplan.org/

Davis, S. M., Gunderson, L. H., Park, W. A., Richardson, J. R., & Mattson, J. E. (1994). Landscape dimension, composition, and function in a changing Everglades ecosystem. In S. M. Davis, & J. C. Ogden (Eds.), *Everglades: the ecosystem and its restoration* (pp. 419–444). Delray Beach, Florida: St Lucie Press.

De Jong, S. M., & van der Meer, F. D. (2004). *Remote sensing image analysis: Including the spatial domain.* : Kluwer Academic Publishers.

Doren, R. F., Rutchey, K., & Welch, R. (1999). The Everglades: A perspective on the requirements and applications for vegetation map and database products. *Photogrammetric Engineering and Remote Sensing*, *65*, 155–161.

Ferro, C., & Warner, T. (2002). Scale and texture in digital image classification. *Photogrammetric Engineering and Remote Sensing*, *68*, 51–63.

Foody, G. M. (2004). Thematic map comparison: Evaluating the statistical significance of differences in classification accuracy. *Photogrammetric Engineering and Remote Sensing*, *70*, 627–633.

Green, A. A., Berman, M., Switzer, P., & Craig, M. D. (1988). A transformation for ordering multispectral data in terms of image quality with implications for noise removal. *IEEE Transactions on Geoscience and Remote Sensing*, *26*, 65–74.

Hall-Beyer, M. (2007). *The GLCM tutorial home page.* Accessed on 12 April 2012 from , http://www.fp.ucalgary.ca/mhallbey/tutorial.htm.

Harken, J., & Sugumaran, R. (2005). Classification of Iowa wetlands using an airborne hyperspectral image: A comparison of the spectral angle mapper classifier and an object-oriented approach. *Canadian Journal of Remote Sensing*, *31*, 167–174.

Held, A., Ticehurst, C., Lymburner, L., & Williams, N. (2003). High resolution mapping of tropical mangrove ecosystems using hyperspectral and radar remote sensing. *International Journal of Remote Sensing*, *24*, 2739–2759.

Hirano, A., Madden, M., & Welch, R. (2003). Hyperspectral image data for mapping wetland vegetation. *Wetlands*, *23*, 436–448.

Huang, C., Davis, L. S., & Townshend, J. R. G. (2002). An assessment of support vector machines for land cover classification. *International Journal of Remote Sensing*, *23*, 725–749.

Hunter, E. L., & Power, C. H. (2002). An assessment of two classification methods for mapping Thames Estuary intertidal habitats using CASI data. *International Journal of Remote Sensing*, *23*, 2989–3008.

Jensen, J. R. (2005). *Introductory digital image processing: A remote sensing perspective* (3rd ed.). Upper Saddle River, NJ: Prentice Hall.

Johnson, B., & Xie, Z. (2011). Unsupervised image segmentation evaluation and refinement using a multi-scale approach. *ISPRS Journal of Photogrammetry and Remote Sensing*, *66*, 473–483.

Jollineau, M. Y., & Howarth, P. J. (2008). Mapping an inland wetland complex using hyperspectral imagery. *International Journal of Remote Sensing*, *29*, 3609–3631.

Jones, J. W. (2011). Remote sensing of vegetation pattern and condition to monitor changes in Everglades biogeochemistry. *Critical Reviews in Environmental Science and Technology*, *41*, 64–91.

Kamal, M., & Phinn, S. (2011). Hyperspectral data for mangrove species mapping: A comparison of pixel-based and object-based approach. *Remote Sensing*, *3*, 2222–2242.

Kim, M., Madden, M., & Warner, T. (2009). Forest type mapping using object-specific texture measures from multispectral ikonos imagery: Segmentation quality and image classification issues. *Photogrammetric Engineering and Remote Sensing*, *75*, 819–829.

Kohonen, T., Hynninen, J., Kangas, J., Laaksonen, J., & Torkkola, K. (1996). *LVQ_PAK: The Learning Vector Quantization Program Package.* Technical report of Helsinki University of Technology, Finland.

Li, L., Ustin, S. L., & Lay, M. (2005). Application of multiple endmember spectral mixture analysis (MESMA) to AVIRIS imagery for coastal salt marsh mapping: A case study in China Camp, CA, USA. *International Journal of Remote Sensing*, *26*, 5193–5207.

Liu, D., & Xia, F. (2010). Assessing object-based classification: Advantages and limitations. *Remote Sensing Letters*, *1*, 187–194.

Madden, M., Jones, D., & Vilchek, L. (1999). Photointerpretation key for the Everglades vegetation classification system. *Photogrammetric Engineering and Remote Sensing*, *65*, 171–177.

Mas, J. F., & Flores, J. J. (2008). The application of artificial neural networks to the analysis of remotely sensed data. *International Journal of Remote Sensing*, *29*, 617–663.

McPherson, B. F., & Halley, R. (1996). *The south Florida environment—A region under stress.* U.S. Geological Survey Circular 1134.

Melgani, F., & Bruzzone, L. (2004). Classification of hyperspectral remote sensing images with support vector machines. *IEEE Transactions on Geoscience and Remote Sensing*, *42*, 1778–1790.

Mountrakis, G., Im, J., & Ogole, C. (2010). Support vector machines in remote sensing: A review. *ISPRS Journal of Photogrammetry and Remote Sensing*, *66*, 247–259.

Pengra, B. W., Johnston, C. A., & Loveland, T. R. (2007). Mapping an invasive plant, *Phragmites australis*, in coastal wetlands using the EO-1 Hyperion hyperspectral sensor. *Remote Sensing of Environment*, *108*, 74–81.

Qiu, F. (2008). Neuro-fuzzy based analysis of hyperspectral imagery. *Photogrammetric Engineering and Remote Sensing*, *74*, 1235–1247.

Qiu, F., & Jensen, J. R. (2004). Opening the black box of neural networks for remote sensing image classification. *International Journal of Remote Sensing*, *25*, 1749–1768.

Rosso, P. H., Ustin, S. L., & Hastings, A. (2005). Mapping marshland vegetation of San Francisco Bay, California, using hyperspectral data. *International Journal of Remote Sensing*, *26*, 5169–5191.

Rutchey, K., Schall, T., & Sklar, F. (2008). Development of vegetation maps for assessing Everglades restoration progress. *Wetlands*, *28*, 806–816.

Rutchey, K., & Vilchek, L. (1999). Air photointerpretation and satellite imagery analysis techniques for mapping cattail coverage in a northern Everglades impoundment. *Photogrammetric Engineering and Remote Sensing*, *65*, 185–191.

Schmidt, K. S., Skidmore, A. K., Kloosterman, E. H., Vanoostern, H., Kumar, L., & Janssen, J. A. M. (2004). Mapping coastal vegetation using an expert system and hyperspectral imagery. *Photogrammetric Engineering and Remote Sensing*, *70*, 703–715.

Trimble (2011). *eCognition Developer 8.64.1 reference book.* .

Villmann, T., Merényi, E., & Hammer, B. (2003). Neural maps in remote sensing image analysis. *Neural Networks*, *16*, 389–403.

Warner, T. (2011). Kernel-based texture in remote sensing image classification. *Geography Compass*, *5*, 781–798.

Welch, R., Madden, M., & Doren, R. F. (1999). Mapping the Everglades. *Photogrammetric Engineering and Remote Sensing*, *65*, 163–170.

Yang, X. (2011). Parameterizing support vector machines for land cover classification. *Photogrammetric Engineering and Remote Sensing*, *77*, 27–37.

Yang, C., Everitt, J. H., & Johnson, H. B. (2009). Applying image transformation and classification techniques to airborne hyperspectral imagery for mapping Ashe juniper infestations. *International Journal of Remote Sensing*, *30*, 2741–2758.

Zhang, C., and F. Qiu, accepted for publication. Mapping individual tree species for an urban forest using airborne LiDAR data and hyperspectral imagery. *Photogrammetric Engineering and Remote Sensing*.